International Journal for Housing Science and Its Applications
Publish August 5, 2025. Volume 46, Issue 3 Pages 3661-3674

https://doi.org/10.70517/ijhsa463309

Analysis of rocky slope destabilization mechanism combining numerical computation and geotechnical mechanics and application for prevention and control

Jiangrui Niu[1,2,*], Yingqiang Su[1,2], Lu Sun[1,2] and Liangliang Chen[1,2]
[1] School of Architectural Engineering, Huzhou Vocational and Technical College, Huzhou, Zhejiang, 313000, China
[2] Huzhou Key Laboratory of Green Building Technology, Huzhou Vocational and Technical College, Huzhou, Zhejiang, 313000, China
Corresponding authors: (e-mail: jrniu_huvtc@163.com).

Abstract Nowadays, computer technology has been developed rapidly, and numerical calculation methods have been widely used in geotechnics. Among them, the finite element method has developed into a powerful computational analysis tool. Based on the basic principle of the finite element strength reduction method, the article constructs the intrinsic model of rocky slope. The implementation process of finite element strength reduction method in ABAQUS for slope stability analysis is discussed. At the same time, we discuss the modeling process of evaluating the stability of jointed rocky slopes in ABAQUS software. Through the analysis of slope stability and destabilization mode, it can be seen that with the decrease of joint spacing s, the density of joints inside the slope increases, the safety coefficient of the slope decreases, and the destabilization mode of the slope is gradually transformed from the logarithmic spiral form to the folded line form. After applying the rocky slope management method of “anchor cable + inclined support wall + anti-slip pile”, the maximum displacement value is only 2.55mm, which indicates that the slope is in a stable state, and the anti-slip key has achieved the expected effect.

Index Terms Strength reduction method, ABAQUS, Geotechnics, Slope management, Numerical calculation

I. Introduction

In the past 10 years, in the face of complex geological disasters, China's disaster prevention and mitigation capabilities have been continuously improved, the construction of a comprehensive disaster prevention capacity system has been continuously improved, the scientific and technological support and leading capacity has been rapidly improved, and the monitoring and early warning has been significantly strengthened [1]. China is one of the countries with the most serious geological disasters and the most threatened population in the world, according to statistics, more than 280,000 potential disaster sites have been identified in China, which cover a population of more than 10 million people and a property of more than 400 billion yuan, of which more than 60% are slope instability and landslides [2], [3]. Under the new situation of disaster prevention and mitigation, the government has put forward the policy of "prevention first, prevention and resistance combined", insisting on the unity of normal disaster reduction and abnormal disaster relief, shifting from post-disaster rescue to pre-disaster prevention, from single disaster to comprehensive disaster reduction, and from disaster loss reduction to disaster risk reduction, so as to comprehensively promote the comprehensive prevention and control of natural disasters in the whole society [4]-[6]. Therefore, for the study of rocky slope stability, it is necessary to correctly understand its destabilization mechanism, explore the perfect slope theory, and manage the potential unstable slopes in a timely and reasonable manner [7]. At the same time, the establishment of perfect and reliable monitoring and early warning judgments, as a way to continuously improve the ability and level of disaster prevention and mitigation, to ensure the safety of people's lives and properties [8].

At present, scholars mainly use the limit equilibrium method, which is widely used in engineering, the finite element strength reduction method, which has been developed rapidly in recent years, and the discontinuous deformation analysis method for the tipping damage for the analysis of slope stability [9]-[11]. Using a combination of limit equilibrium analysis and numerical simulation, Sengani and Mulenga [12] investigated the common factors responsible for geotechnical slope instability and found that unstable slopes are associated with slip-type dumping, and are also controlled by tensile cracks and laminated soils. Garo et al [13] used the finite element method and limit equilibrium method to model slope stability and found that due to rainfall and seismic activity, slopes can be in an unstable condition. Dyson and Tolooiyan [14] utilized a combination of FORTRAN and Python codes to implement the strength discounting finite element method through a computer-aided engineering package (Abaqus), which is effective in estimating the factor of safety for slope stability. Tschuchnigg et al [15] investigated the rocky

slope instability mechanism by means of finite element limit analysis and strength discounted finite element analysis, which showed that the main advantage of limit analysis is that the FoS value can be defined by upper and lower limit calculations.

The form of damage in geotechnical bodies is usually shear damage, and most of the existing methods for slope stability analysis use whether or not overall Moore-Coulomb shear damage occurs within the geotechnical body along the sliding surface as a criterion for discrimination [16]. Luo et al [17] analyzed slope stability using a modified Mohr-Coulomb damage criterion that considers both shear and tension damage mechanisms. Aksoy et al [18] compared the application of Hoek-Brown damage criterion and Mohr-Coulomb damage criterion in numerical simulation for slope stability analysis of a deep open pit mine, which had experienced two major landslides. Yerro et al [19] used the strain-softened Mohr-Coulomb model and progressive failure mechanism to study slope instability and post-failure behavior, and simulated the internal kinematics and degradation of rocky slope sliding bodies using the material point method (MPM). Dai et al [20] introduced the Barton-Bandis (B-B) nonlinear strength criterion to improve the Mohr-Coulomb model for analyzing the stability of rocky slopes affected by a discontinuous surface, and the results showed that the improved model could better reflect the real-time shear strength.

The article firstly introduces the finite element numerical calculation methods such as the strength reduction theory and the principal model. Subsequently, it explores the implementation process of finite element strength reduction method in slope stability analysis in ABAQUS software. The nonlinear finite element method is utilized in ABAQUS software for the solution. Subsequently, the stability calculation of nodular rocky slopes is implemented in ABAQUS using the intensity discount method, and a detailed modeling process is provided. Taking a slope as an example, the application of finite element simulation in the stability of nodular rocky slopes is discussed, and the positive significance of finite element simulation in slope stability evaluation is discussed. Based on the constructed model, the effects of joint inclination, joint spacing, joint connectivity and the number of joint groups on slope stability are investigated. Finally, the slope management method of “anchor cable + inclined support wall + anti-slip pile” is proposed.

II. Numerical calculation and analysis methods for slopes

II. A. Brief description of finite element numerical calculation methods

II. A. 1) Theory of strength reduction

Strength discount method: by gradually reducing the shear strength (c,ϕ) until the design can not converge, will not be able to converge the stage is considered as destruction, the maximum strength discount rate of this stage as the slope minimum stability factor. When the slope stability coefficient is calculated, the stress state of any unit Gaussian point A on the slope is firstly expressed by Mohr's circle, and the shear strength envelope is shown in Fig. 1. To simulate the damage state of the slope, the Mohr's circle of the stress state on the assumed damage surface needs to be close to the damage envelope [21]. A factor of safety F divided by the shear strength at point A is first assumed to be close to the Mohr's circle, i.e., the stress state at that point is corrected to the damage state. The slope will be damaged as a whole with the increase of damage points, and the finite element analysis will be dispersed, at which time the value of the safety factor F is the minimum safety factor.

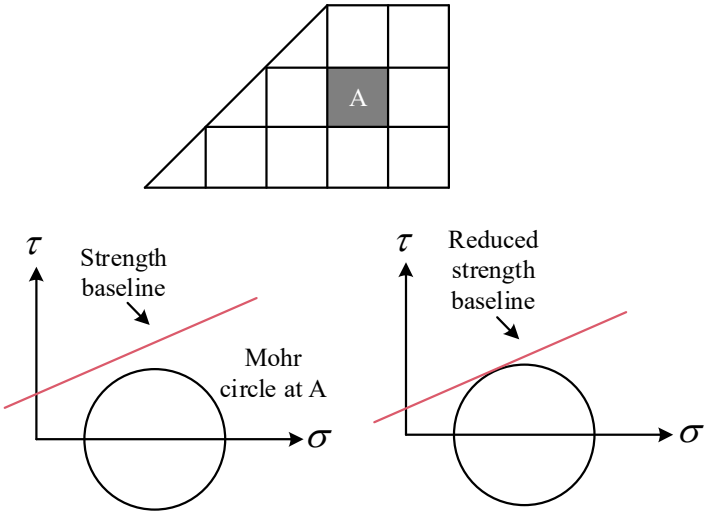

Figure 1: Shear strength envelope

Using this method in the calculation of the minimum factor of safety, assuming that the Poisson's ratio v and the modulus of elasticity E of the slope remain unchanged, the angle of internal friction ϕ and the cohesion c are gradually reduced in the following manner until the calculation of the termination at the time of the dispersion, at which time F is the minimum factor of safety. Factor of safety formula for slope failure:

$$F_s = \frac{\tau}{\tau_f} \tag{1}$$

where: τ : shear strength of the slope:

$$\tau = c + \sigma_n \tan\phi \tag{2}$$

τ_f : Shear stress on the sliding surface:

$$\tau_f = c_f + \sigma_n \tan\phi_f \tag{3}$$

Let the strength discount factor be SRF, at which point the shear strength factor is: $c_f = \frac{c}{SRF}, \phi_f = \tan^{-1}(\frac{\tan\phi}{SRF})$.

Increasing Fs by a very small amount will increase the computation time, but will result in an accurate minimum stability factor [22].

II. A. 2) Ontological model

Since geotechnical bodies are not isotropic materials, stress levels, and force processes affect the stress-strain relationship of geotechnical bodies, it is very difficult to choose a mathematical model that can comprehensively and correctly reflect these complex relationships. Therefore, special soil bodies, special engineering objects and problem characteristics should be studied, and mathematical models should be established for the main characteristics of the research problem.

The shear strength determines the stability of geotechnical bodies, and the shear and elastic properties determine the deformation capacity. When the loading is greater than the geotechnical shear strength, the geotechnical soil will produce a plastic region, and with the development of the plastic region it will reach a state of destruction. The plastic region does not mean that the structure must be unstable, because the plastic region is surrounded by the elastic region will not be able to generate the damage surface, then the local damage may not develop into a whole damage. The total strain generated under load includes: elastic strain and plastic strain:

$$\varepsilon = \varepsilon^e + \varepsilon^p \tag{4}$$

Among them, ε - total strain, ε^e - elastic strain, ε^p - plastic strain.

The Moore-Cullen model is used for slope stability analysis in MIDAS-GTS finite element analysis software. The main calculation parameters: modulus of elasticity E, cohesion C, angle of internal friction φ, bulk weight γ and tensile strength of the geotechnical body.

(1) Yield function

The expression for the strength criterion of the M-C model is:

$$\sigma_1 = \sigma_3 \tan^2(45° + \frac{\varphi}{2}) + 2c\tan(45° + \frac{\varphi}{2}) \tag{5}$$

If the stress invariant representation is used:

$$\frac{I_1}{3}\sin\varphi - \sqrt{J_2}\left[\frac{1}{\sqrt{3}}\sin\theta\sin\varphi + \cos\theta\right] + c\cos\varphi = 0 \tag{6}$$

where: I_1 is the first stress invariant, $I_1 = \sigma_1 + \sigma_2 + \sigma_3$.

J_2 is the second stress invariant, $J_2 = \frac{1}{6}\left[(\sigma_1 - \sigma_2)^2 + (\sigma_2 - \sigma_3)^2 + (\sigma_3 - \sigma_1)^2\right]$.

The Moore-Coulomb strength criterion is an irregular hexagonal surface in principal stress space. Its cross-sectional shape in the π plane is an irregular hexagon. The M-C model yield surface is an angular conical surface whose corner points are extremely inconvenient for numerical calculations. In order to obtain a smooth yield surface that approximates the M-C surface, Drucker-Prager modified the Mises criterion and proposed the D-P criterion, viz:

$$F = \alpha I_1 + \sqrt{J_2} - k = 0 \tag{7}$$

where: α, k is the material constant.

The yield surface of the D-P model is a positive conic surface [23]. Its cross-sectional shape in the π plane is circular, and taking the appropriate material try, α, k, can make the D-P yield surface close to the M-C yield surface. If one takes Eq:

$$\alpha = \frac{2\sin\varphi}{(3-\sin\varphi)\sqrt{3}} \tag{8}$$

$$k = \frac{6c\cos\varphi}{\sqrt{3}(3-\sin\varphi)} \tag{9}$$

Then the D-P yield circle coincides with the outer vertices of the M-C hexagon. If taken:

$$\alpha = \frac{2\sin\varphi}{(3+\sin\varphi)\sqrt{3}} \tag{10}$$

$$k = \frac{6\cos\varphi}{\sqrt{3}(3+\sin\varphi)} \tag{11}$$

Then the D-P yield circle coincides with the inner vertex of the M-C hexagon.

(2) Hardening criterion

The hardening criterion describes the way in which the subsequent yield surface of a material in the plastic region changes with the development of plastic strain in the principal stress space, thereby determining the state of stress in the plastic region. Ideally, the yield surface of an elastoplastic material will remain unchanged after it enters the plastic state. Different materials have their own development of material properties after yielding, and the relationship between hardening, softening and ideal materials is shown in Figure 2.

The following two models are used for geotechnical body materials:

(a) Isotropic strengthening model

A simplified model with equal strength in any loading direction, the loading surface is the yield surface similarly expanded, and the subsequent yield surface develops from the uniform expansion of the initial yield surface.

(b) Follower strengthening model

Simplified model considering the Bauschinger effect: the degree of strengthening in one loading direction is equal to the degree of weakening in the opposite direction, and the subsequent yield surface translates in the principal stress space.

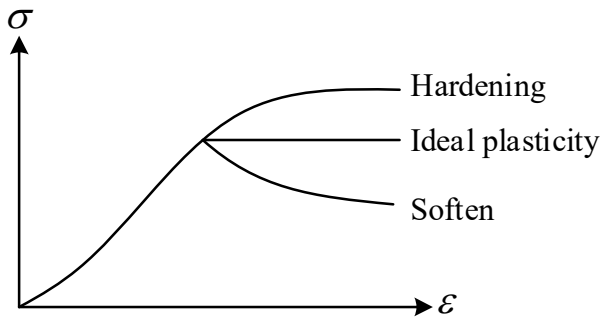

Figure 2: Relationship between hardening, Softening and ideal materials

The isotropic hardened yield surface has a constant center and shape, and its size varies with the hardening parameters. Geotechnical materials are hardened materials where the yield surface expands uniformly with increasing plastic strain. Softened material yield surface can be reduced, isotropic hardening similar to plastic deformation isotropic as a prerequisite.

(3) Flow law

The plastic strain increment $d\varepsilon_{ij}^{p}$ of an elastoplastic material has the following relationship with the plastic potential function g:

$$d\varepsilon_{ij}^{p} = d\lambda \frac{\partial g}{\partial \sigma_{ij}} \tag{12}$$

where: $d\lambda$ is some pending non-negative scale parameter. If the plastic potential function is the yield function, i.e., $g = f$, then:

$$d\varepsilon_{ij}^{p} = d\lambda \frac{\partial f}{\partial \sigma_{ij}} \tag{13}$$

In general, the relationship given by $g \neq f$, Eq. is called the non-associative flow law. Eq. is called the associated plastic flow law. Most geotechnical materials, concrete materials, its plastic deformation characteristics of non-associated, theoretically in the calculation should be used in the non-associated flow law. However, in the elastic-plasticity theory solution, in order to make the material deformation stable development, to get the elastic-plasticity matrix $\{d\varepsilon^{p}\}$ symmetry, in general, can be used to associate the flow law.

(4) Addition and deletion of units

The initial stress state of the added unit in the construction phase analysis is zero, and the geotechnical unit is in a stressed state before deletion. If the deleted unit around the original load, the remaining units through the stress relief so that the newly generated free surface is not subject to the action of stress. The load assignment of the deleted unit is shown in Fig. 3, where A is deleted from B. The stresses of A and B before deletion are σ_{AO} and σ_{BO}, respectively, and all the loads generating this stress are considered. Since the two objects are in equilibrium, the load F_{AB} should be applied from A to B in order to maintain equilibrium with σ_{BO}. Similarly the load F_{BA} should act on A. Thus the excavation load acting on a boundary, the stress state of an excavation unit is related to the self-weight of that unit. The following equation can be defined:

$$F_{BA} = -\int_{V_A} B^{T} \sigma_{AO} dV_A + \int_{V_A} N^{T} \gamma dV_A \tag{14}$$

Where, B - strain-displacement relationship matrix, V_A - excavation volume, N - cell shape function.
γ - volumetric weight of the rock and soil.

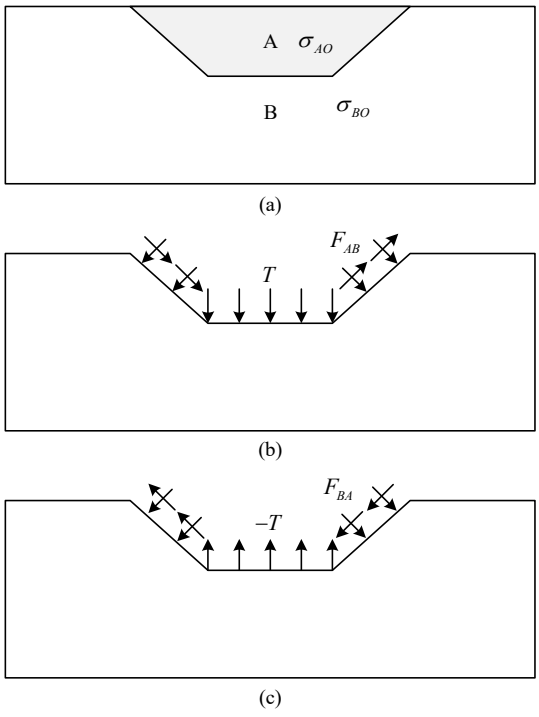

Figure 3: Schematic diagram of load distribution of the deleted unit

II. B.Implementation of slope stability analysis in ABAQUS

II. B. 1) Introduction to ABAQUS Software

ABAQUS is a powerful general-purpose finite element software, which contains rich material models, unit modes, loads and boundary conditions, and is capable of solving a variety of static, dynamic and other problems, and has good applicability to nonlinear problems, so it is more suitable for slope stability analysis.

ABAQUS software system is mainly composed of pre- and post-processing module, general analysis module, special analysis module and interface module with third-party software. The pre- and post-processing module of ABAQUS/CAE provides an interactive graphical user interface with powerful pre- and post-processing functions, including the entire process of analysis. The analysis results can be finally output with curves, cloud diagrams and other images. General analysis module mainly consists of ABAQUS/ Standard, which can be used to analyze most of the linear and nonlinear problems, and ABAQUS/CFD, which adopts ABAQUS/Explicit, which displays the dynamic finite element format for fluid dynamics analysis. Dedicated modules provide specialized analyses for industry-specific problems, such as marine structures. Interfaces to third-party software ABAQUS provides a geometry interface module to exchange data with geometry models generated by third-party CAD software.

II. B. 2) Implementation of Finite Element Strength Reduction Method in ABAQUS

The essence of the finite element strength discount method is the process of gradually reducing the value of the shear strength parameter c,φ of the geotechnical body, so that the stress in a unit of the geotechnical body exceeds the strength range, or exceeds the yield surface, and thus spreads to the other surrounding geotechnical bodies. In this process of continuous diffusion, the slope is destabilized when its yielding unit body forms a through slip surface in the slope body [24]. In ABAQUS, the process of decreasing the strength parameters of geotechnical bodies can be controlled by field variables in the following steps:

(1) Define a field variable, i.e., the strength discount factor F_s.

(2) Define the geotechnical material model parameters that vary with the strength discount factor F_s.

(3) Specify the magnitude of the strength discount factor F_s at the beginning of the analysis and assign gravity loads to the modeling and establish the equilibrium stress state. In order to avoid damage at the initial moment, F_s is taken to a smaller value, e.g., $F_s<1$ at the beginning, i.e., to expand the strength of the material model.

(4) The strength discount factor F_S is increased linearly in the subsequent analysis step, and the results are processed after the computation is aborted, and the stabilization coefficient is determined in accordance with the instability evaluation criteria.

II. B. 3) Nonlinear finite element solution methods in ABAQUS software

The nonlinear finite element solution equation is expressed in the form:

$$f(u)=0 \tag{15}$$

where f and u are vectors, which can be interpreted as forces and displacements for mechanical problems. The equation is solved in ABAQUS/Standard using the Newton iterative method. Let an approximate solution u_i ($f(u_i)\neq 0$, abbreviated as $\hat{f}$) has been obtained after the i th iteration, and its difference with the exact solution is w_{i+1}. Then there should be:

$$f(u_i+w_{i+1})=0 \tag{16}$$

Expanding Eq. by Taylor's formula and removing the higher order terms yields:

$$Kw_{i+1}=-f_i \tag{17}$$

where $K_i=\dfrac{\partial f}{\partial u}(u=u_i)$ is the Jacobia stiffness matrix.

If w_{i+1} is obtained from the formula, then the next-level iterative displacement u_{i+1} is:

$$u_{i+1}=u_i+w_{i+1} \tag{18}$$

By repeating the iterative method, it is determined whether the computation converges or not based on f_i and w_{i+1}. For general nonlinear problems, the Newton iterative method usually gives good results. In the generation and inverse of the stiffness matrix, it usually requires larger computational resources, at this time, you can also consider the proposed Newton (mN-R) method, that is, the same stiffness matrix is used in the iterative process, and no

longer generate and inverse the calculation at each step, although this practice will reduce the convergence speed, but the iterative process is more realistic solution.

III. ABAQUS finite element modeling

III. A. Criteria for determining instability

Slope instability criterion is the key to the finite element strength discount method, and there are mainly 2 kinds of slope instability criterion in finite element analysis:

(1) The strength parameter of the rock mass after discounting no longer converges within the specified number of iterations.

(2) There is a plastic zone from the slope surface to the top of the slope. Finite element numerical computation does not converge must indicate that the plastic zone through or displacement of the sudden change, while the plastic zone through is only a necessary condition of slope instability, plastic zone through, need to further observe the displacement of the slope mass point. In this paper, we will use the iterative non-convergence combined with the plastic zone penetration and obvious displacement of the two criteria to analyze the slope instability.

III. B. Modeling process

The steps for modeling a solid in ABAQUS software are: create the part → create the cross-section material and cross-section features → assemble the part → define the analysis step → establish the interactions → define the loads and boundary conditions → meshing → submit the task → visualize the operation.

III. B. 1) Creating components

In the component module, enter the graphic editing interface to draw the geometric contours of the slope according to the measured profile, or directly import the *DXF file created by CAD.

After the slope profile is drawn, the relative position of the joint group and the rock block is established according to the measured situation. The rock blocks and knuckle components are shown in Figure 4. After intersecting in the profile, the slope is divided into eight rock blocks, and sets are established for the nodal groups and rock blocks respectively, with the purpose of facilitating the subsequent uniform assignment of component attributes.

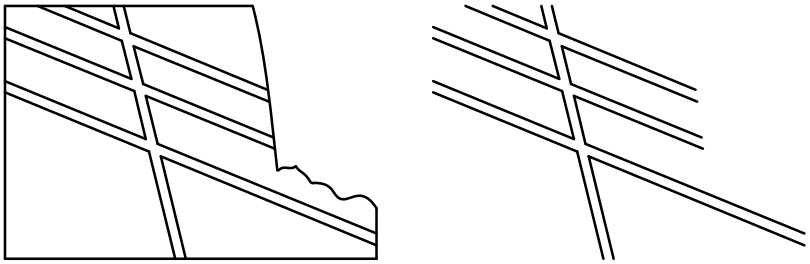

Figure 4: Diagram of rock blocks and joint components

III. B. 2) Creating Section Materials and Section Features

In the properties module, the material properties of joints and rock masses are established respectively. The destruction of the rock mass is a gradual process, from the initial elastic state to plastic flow, and finally reaches the ultimate state of destruction, so the rock mass has both elastic and plastic characteristics. The modulus of elasticity and Poisson's ratio of the nodule group and the rock mass are entered in the elasticity setting, and the variation of the cohesion and the angle of internal friction of the two materials with respect to the field variables needs to be specified in the Mohr-Coulomb plasticity setting. Into the Moore-Coulomb plasticity command box, the number of field variables is set to 1, and then in the plastic part of the strength reduction formula based on the internal friction angle and shear expansion angle with the change of field variables, field variables at this time that is the significance of the strength reduction coefficient, the initial value of the initial value of less than 1 in general, in order to amplify the strength, to facilitate the search for the limit of the damage state. This example will be set to the initial value of 0.5, take a linear increase in the way of segmented linear simulation, the increment is 0.25, the final value of 3. As mentioned above, do not take into account the volumetric deformation of the slope, so the shear angle of expansion is taken as zero. Similarly, the cohesive force, which varies with the field variables, is set based on the strength discount equation. In particular, no units are specified in ABAQUS, and the user only needs to ensure that the selected units are harmonized, e.g. by using the International System of Units (SI).

III. B. 3) Assembly of components

In this module, the knuckle group is assembled with each rock block, up to which point the previously separately operated components are unified into a common interface.

III. B. 4) Defining the analysis step

A generic static analysis step was created and the initial incremental step was changed from 1 to 0.1 with the purpose of convergence by decreasing the initial incremental step so that the number of iterations increases. In the equation solver set the matrix storage to asymmetric analysis, the reason for choosing asymmetric analysis is that the Mohr-Coulomb eigenstructure model in ABAQUS uses a non-associative flow law, the yield surface and the plastic potential surface are different, so the stiffness matrix is not symmetric and has to be solved with an asymmetric solver.

III. B. 5) Establishment of interactions

First define the individual contact surfaces. Master surfaces are defined in the manager, and slave surfaces are defined afterwards. The definition of master and slave surfaces generally follows: the fine mesh is used as the slave surface, and the less rigid surface is used as the slave surface. In the example, the surface of the rock block is used as the master surface, and the nodal surface is used as the slave surface.

In this module, Instance & Create is executed to assemble the nodal group with each rock block, so that the previously separately operated components are unified into a common operation interface.

Next, the contact properties with friction are defined. In the contact properties option, the tangential and normal behaviors in mechanics are loaded, and the normal behavior is set to hard contact. For the tangential behavior, the coefficient of static-dynamic friction is set in the Static Friction - Dynamic Friction Coefficient option.

Finally define the contact pairs. Set the analysis step to the initial state, indicating that the contact has existed since the initial state, and then select the master surface, followed by the slave surface, to establish the contact pairs between the rock mass and the joint group, respectively.

III. B. 6) Defining loads and boundary conditions

Set the initial state analysis step category as Mechanical, type as Displacement/turning angle, and then after selecting the left and right boundaries in the example except the slope surface, check U1 in the pop-up boundary condition editor in order to limit the translational degree of freedom of the example along the X-axis direction. Similarly, create the boundary conditions again, select the bottom boundary and then check U1 and U2 in the pop-up boundary condition editor in order to limit the translational degrees of freedom of the example along the X and Y axes.

III. B. 7) Gridding

The components are meshed in the grid module to discretize the continuous rock mass and joint system into a finite number of cells.

III. B. 8) Controlling changes in field variables

Edit the model's keywords in the left model tree to control field variable changes. Use the *Initialconditions in conjunction with the *Field command, setting type=field in the former command to define the initial value of the field variable. Locate the first analysis step statement, "*Step, name=load, nlgeom=NO, unsymm=YES", and enter before it, after the dotted line:

*Initialconditions, type=field, variable=1

slope-1. set-1, 0.5

Locate the second analysis step statement "*Step, name=reduce, nlgeom=NO, unsymm=YES" and enter the following command after it:

*Field, VARIABLE=1

slope-l.set-1, 3

where "slope-1.set-1" is the name of the point set of the discounted part, which in the example is the point set of the nodal group, and the name of the point set can be located manually from the assembly module of the model tree.

IV. Example analysis and proposal of application methods for prevention and control

IV. A. Examples of Finite Element Models

The model is based on a provincial open-pit mine on one of the high slopes after simplification, the model slope height of 120m, the modulus of elasticity is 1GPa, Poisson's ratio is 0.25, the cohesion is 0.5MPa, the angle of internal friction is 30 °, the density of the rock and soil body is 2400 kg/m³, and the angle of the slope is 45°. Slope

calculation according to the plane strain to establish a finite element model, the boundary conditions for the left and right sides of the horizontal constraints, the lower part of the fixed, the upper part of the free boundary, a one-time application of all the gravity load, that is, the load increment step is set to 1 step. The finite element solver is the sparse matrix solver provided by ANSYS, and the full Newton-Raphson iteration method is selected, in which the stiffness matrix is modified once for each equilibrium iteration, and the maximum number of iterations is 500. 980 cells are used in this model. The correspondence between the example discount factor and the cohesion and internal friction angle is shown in Table 1.

Table 1: The calculation example of the reduction coefficient is corresponding

Folding coefficient	c'/MPa	$\varphi'/°$
1.0	0.517	30
2.0	0.234	16.27
2.5	0.165	13.25
2.7	0.176	12.14
2.8	0.173	11.64
3.0	0.142	10.94
3.1	0.16	10.22
3.2	0.156	10.51

The strain maps of the plastic zone when the discount factor is 2, 3 and 3.2 are shown in Fig. 5 to Fig. 7. It can be understood that the whole process of the development of the plastic zone of the slope until the penetration of the slope, when the discount factor of 3 slope model calculation does not converge, and at this time the foot of the slope in the horizontal direction there is a sudden change in displacement.

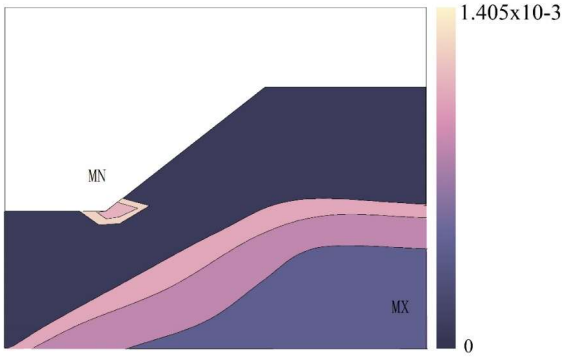

Figure 5: The deformation of the plastic zone of the plastic zone is 2

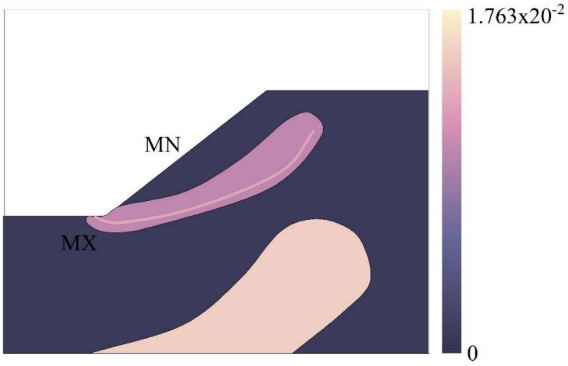

Figure 6: The deformation of the plastic zone of the plastic zone is 3

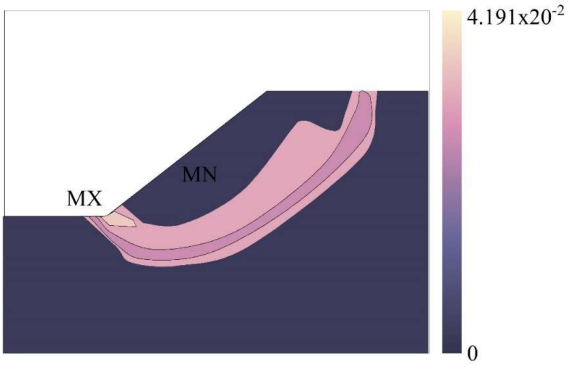

Figure 7: The deformation of the plastic zone of the plastic zone is 3.2

IV. B. Analysis of slope stability and destabilization mode

IV. B. 1) Effect of Nodal Inclination on Slope Stability

In order to investigate the effects of slow-dipping nodal inclination dip_1 and steep-dipping nodal inclination dip_2 on the destabilization mode and stability of rocky slopes, the geometric parameters of the nodal inclination under different nodal inclinations are shown in Table 2.

Table 2: The geometrical parameters of the joint by different joint Angle

s/m	l/m	k	$dip_1/(^\circ)$			$dip_2/(^\circ)$
1	2	0.5	10	20	30	50
1	2	0.5	10	20	30	70
1	2	0.5	10	20	30	90

The geometric parameters of the table joints are inputted into Phase2 numerical simulation software, and the stability analysis of the slopes is carried out by using the finite element strength discounting method, and the change of the safety coefficient of rocky slopes containing two groups of joints F_s with the inclination angle of joints is shown in Fig. 8, and it can be seen from the figure that, as the inclination angle of the gently sloping joints dip_1 increases, the safety coefficient of the slopes generally shows a decreasing trend. The area of the destabilized area of the slope shows a decreasing trend, which is mainly manifested in the decrease of the area of the destabilized area near the foot of the slope, because the increase of dip_1 leads to the area near the slope surface is more unstable, and the slide is more likely to be destabilized at the slope surface. With the increase of steeply dipping nodal inclination dip_2, the slope safety coefficient generally tends to decrease. The destabilization region of the slope extends horizontally near the top of the slope and shortens horizontally near the foot of the slope.

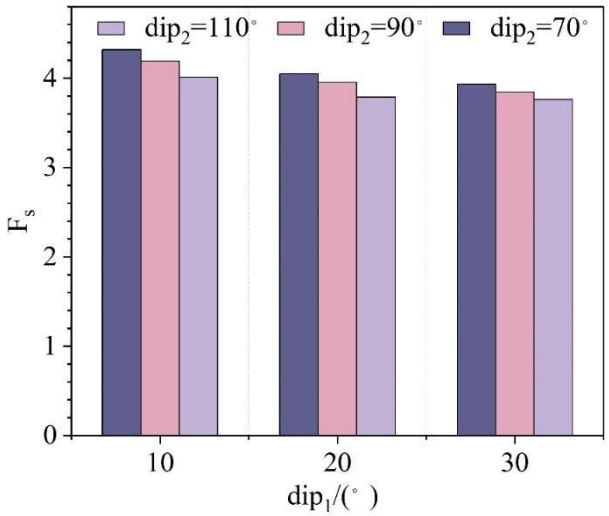

Figure 8: The safety coefficient varies with the Angle of the joint

IV. B. 2) Effect of joint spacing on slope stability

In order to investigate the effect of joint spacing on slope stability and destabilization mode, the geometric parameters of joints with different joint spacing are shown in Table 3.

Table 3: The geometric parameters of the joint spacing

dip_1 /(°)	dip_2 /(°)	l/m	k	s/m
25	100	1	0.5	0.55
25	100	1	0.5	0.7
25	100	1	0.5	1.05
25	100	1	0.5	1.2
25	100	1	0.5	1.55

Through numerical simulation, the change rule of safety coefficient with joint spacing is shown in Fig. 9. As can be seen from the figure, with the decrease of joint spacing, the safety coefficient of the slope gradually decreases, and the decrease amplitude gradually increases, at the same time, the density of the internal joints of the rocky slope increases sharply. Since the mechanical parameters of the joints are smaller than those of the intact rock, the slope is more likely to produce larger displacement and slide near the slope surface, and the instability mode of the slope is more easily affected by the joints. As a result, the destabilization pattern of the slope is gradually transformed from logarithmic spiral form to folded line form.

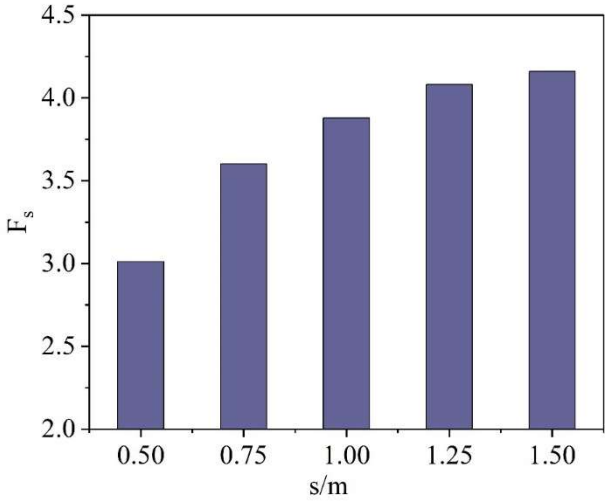

Figure 9: The safety coefficient varies with the spacing of the joint

IV. B. 3) Effect of nodal connectivity on slope stability

Joint connectivity reflects the development of internal joints in rocky slopes, which also has a great influence on slope stability. Therefore, this section investigates the effect of joint connectivity on slope stability and destabilization mode. The geometric parameters of joints with different joint connectivity are shown in Table 4.

Table 4: The geometric parameters of the joint ratio are obtained

dip_1 /(°)	dip_2 /(°)	s/m	k					l/m
25	100	1	0.5	0.6	0.7	0.8	0.9	2
25	100	1	0.5	0.6	0.7	0.8	0.9	3
25	100	1	0.5	0.6	0.7	0.8	0.9	4

After calculation, the change rule of slope safety coefficient with nodal connectivity is shown in Fig. 10. From the figure, it can be seen that with the increase of nodal connectivity, the safety coefficient of slope decreases gradually. In addition, when the connectivity of the joints is the same, the longer the length of the joints, the lower the safety coefficient of the slope. When the connectivity of joints k =1.0, the joints inside the slope are transformed from non-through joints to through joints, and then the safety coefficient of the slope is only 1.32, which makes the through-jointed rocky slope more unstable compared with the non-through-jointed rocky slope.

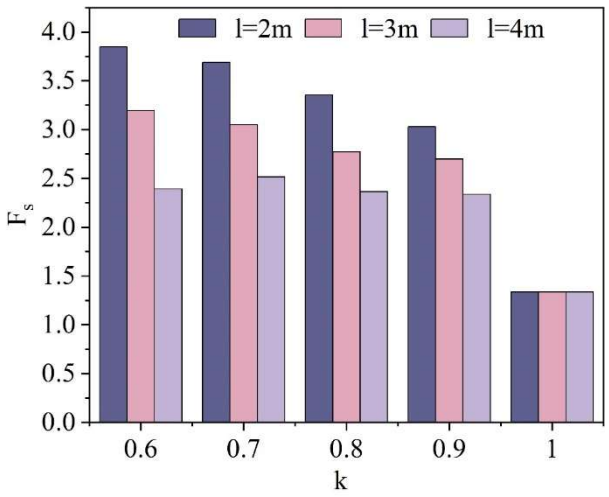

Figure 10: The safety coefficient changes the law of the connecting rate

IV. B. 4) Effect of the number of nodal groups on slope stability

In order to investigate the differences in stability and instability patterns between steep-gently dipping combined jointed rocky slopes and gently dipping jointed rocky slopes, a model containing only one set of gently dipping jointed rocky slopes is constructed in this section. The comparison of the factor of safety of steep-gently dipping combination joints and gently dipping joints slopes is shown in Fig. 11. From the figure, it can be seen that the safety factor of the slope gradually decreases with the increase of the nodal inclination, and the magnitude of the decrease gradually decreases. Compared with the steep-gentle combination joints rocky slope, the rocky slope with only gentle inclination joints is more stable, and the existence of steep inclination joints weakens the geotechnical body inside the slope, and the steep-gentle combination joints rocky slope is more unstable.

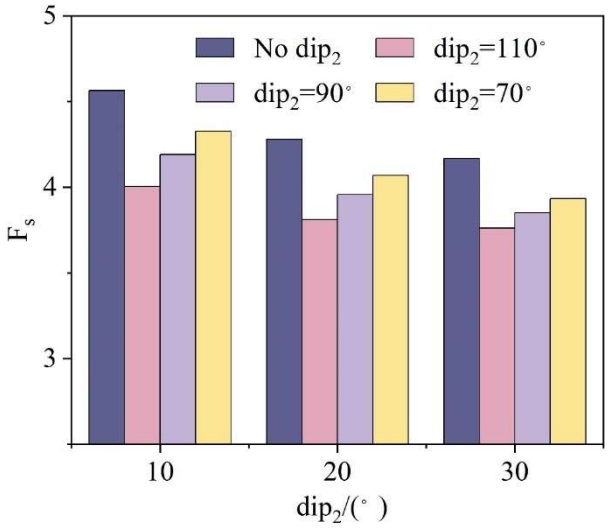

Figure 11: The comparison of the safety coefficient of the steep and slow slope joint slope

IV. C. Reinforcement measures for rocky slopes

IV. C. 1) Reinforcement measures

Combined with the site conditions, referring to the experience of similar projects in the same region, after the program selection, the selected reinforcement measure is the anti-slip key at the foot of the slope, i.e. “Anchor cable + diagonal support wall + anti-slip pile”. The anti-slip key has a depth of 3m, a total length of 9m, a circular cross-section and a radius of 1.5 m. This solution can quickly and effectively improve the safety of the sandstone hazardous rock body and ensure the stability of the slope, but in order to stabilize the slope and the safety of road traffic, it is necessary to carry out safety monitoring and control of the slope to keep abreast of the slope status.

IV. C. 2) Deformation pattern after slope stabilization

Calculation results before reinforcement and field measured data over time as shown in Figure 12 (a ~ c are measurement point 1, measurement point 2 and measurement point 3, respectively). As can be seen from the figure, the three monitoring points of the displacement value over time is basically the same rule of change, are the first to become larger and then tend to a stable value, the maximum displacement value of the three monitoring points are smaller, monitoring point 1, 2, 3 of the maximum displacement value of the measured value of 1.05, 1.93, 2.55mm, respectively, to meet the safety requirements, indicating that the anti-slip key structure plays a more satisfactory effect of the slope reinforcement.

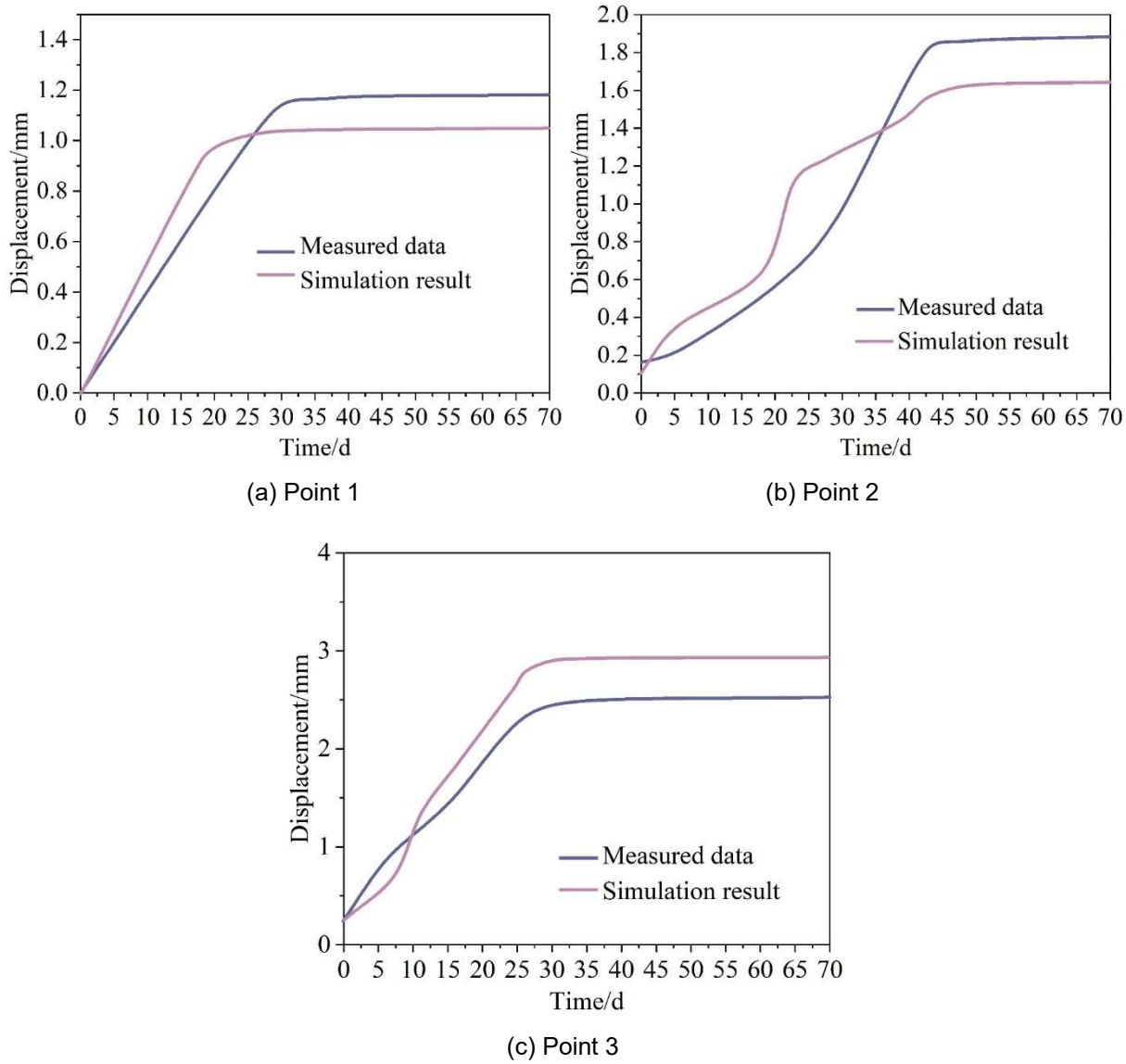

(a) Point 1

(b) Point 2

(c) Point 3

Figure 12: The results of the reinforcement and the actual data are changed at any time

V. Conclusion

The use of finite element strength reduction method can be very effective in simulating the whole process of slope instability, which is of great significance in guiding the analysis of the instability mechanism of rocky slopes and the application of prevention and control. Combined with specific examples, the article empirically investigates the numerical calculation method of slope proposed in this paper and puts forward prevention and control measures.

(1) With the increase of nodal inclination dip_1 and dip_2, the safety coefficient of the slope gradually decreases. The area of the destabilized area of the slope decreases with the increase of dip_1, and the area of the destabilized area near the top of the slope increases while the area of the destabilized area near the foot of the slope decreases with the increase of dip_2.

(2) After applying the rocky slope management method of “anchor cable + inclined support wall + anti-slip pile” proposed in this paper, the deformation of the reinforced slope is small, and the maximum displacement value is less than 3mm, which proves that the anti-slip key has a better reinforcing effect.

Funding

This work was supported by A Project Supported by Scientific Research Fund of Zhejiang Provincial Education Department (Y202250561), and the Talents Foundation of Huzhou Vocational and Technical College.

References

[1] Chen, W., Zhong, C., Qin, X., & Wang, L. (2023). Geological Disaster: An overview. Intelligent Interpretation for Geological Disasters: From Space-Air-Ground Integration Perspective, 1-23.
[2] Zhang, X., Li, Y., Liu, Y., Huang, Y., Wang, Y., & Lu, Z. (2021). Characteristics and prevention mechanisms of artificial slope instability in the Chinese Loess Plateau. Catena, 207, 105621.
[3] He, Y., Li, B., & Du, X. (2023). Soil slope instability mechanism and treatment measures under rainfall—A case study of a slope in Yunda Road. Sustainability, 15(2), 1287.
[4] Chai, J., & Wu, H. Z. (2023). Prevention/mitigation of natural disasters in urban areas. Smart Construction and Sustainable Cities, 1(1), 4.
[5] Liu, X., Lü, X., Shao, Y., Chen, C., Liu, G., Li, Y., ... & Chen, Y. (2024). Monitoring and disaster prevention of high and steep sandstone slopes along highways under construction. Frontiers in Earth Science, 12, 1444592.
[6] Hong-In, P., Takahashi, A., & Likitlersuang, S. (2024). Engineering and environmental assessment of soilbag-based slope stabilisation for sustainable landslide mitigation in mountainous area. Journal of environmental management, 359, 120970.
[7] Park, D. (2023). Stability evaluation of rock slopes with cracks using limit analysis. Rock Mechanics and Rock Engineering, 56(7), 4779-4797.
[8] Zhong, J. H., & Yang, X. L. (2022). Pseudo-dynamic stability of rock slope considering Hoek–Brown strength criterion. Acta Geotechnica, 17(6), 2481-2494.
[9] Liu, S. Y., Shao, L. T., & Li, H. J. (2015). Slope stability analysis using the limit equilibrium method and two finite element methods. Computers and Geotechnics, 63, 291-298.
[10] Arvin, M. R., Zakeri, A., & Bahmani Shoorijeh, M. (2019). Using finite element strength reduction method for stability analysis of geocell-reinforced slopes. Geotechnical and Geological Engineering, 37, 1453-1467.
[11] Yagoda-Biran, G., & Hatzor, Y. H. (2016). Benchmarking the numerical discontinuous deformation analysis method. Computers and Geotechnics, 71, 30-46.
[12] Sengani, F., & Mulenga, F. (2020). Application of limit equilibrium analysis and numerical modeling in a case of slope instability. Sustainability, 12(21), 8870.
[13] Garo, T., Tesfaye, M., & Karuppannan, S. (2024). Slope stability modeling using limit equilibrium and finite element methods: a case study of the Adama City, Northern Main Ethiopian Rift. Quaternary Science Advances, 15, 100228.
[14] Dyson, A. P., & Tolooiyan, A. (2018). Optimisation of strength reduction finite element method codes for slope stability analysis. Innovative Infrastructure Solutions, 3(1), 38.
[15] Tschuchnigg, F., Schweiger, H. F., & Sloan, S. W. (2015). Slope stability analysis by means of finite element limit analysis and finite element strength reduction techniques. Part II: Back analyses of a case history. Computers and Geotechnics, 70, 178-189.
[16] Melentijević, S., Berisavljević, Z., Berisavljević, D., & Marañón, C. O. (2024). Rock slope stability analysis under Hoek–Brown failure criterion with different flow rules. Bulletin of Engineering Geology and the Environment, 83(5), 181.
[17] Luo, W., Li, J., Tang, G., Chen, J., & Dai, C. (2021). Upper-bound limit analysis for slope stability based on modified Mohr–Coulomb failure criterion with tensile cutoff. International Journal of Geomechanics, 21(10), 04021184.
[18] Aksoy, C. O., Uyar, G. G., & Ozcelik, Y. (2016). Comparison of Hoek-Brown and Mohr-Coulomb failure criterion for deep open coal mine slope stability. Structural Engineering and Mechanics, 60(5), 809-828.
[19] Yerro, A., Pinyol, N. M., & Alonso, E. E. (2016). Internal progressive failure in deep-seated landslides. Rock Mechanics and Rock Engineering, 49, 2317-2332.
[20] Dai, Z., Wang, L., Zhang, K., Wang, L., & Gao, X. (2022). Implementation of the Barton–Bandis nonlinear strength criterion into Mohr–Coulomb sliding failure model. Advances in Materials Science and Engineering, 2022(1), 1590884.
[21] Zi-zhen Liu,Zhi-xin Yan & Jian Duan. (2008). Couple analysis on strength reduction theory and rheological mechanism for slope stability. Journal of Central South University of Technology,15(1s),351-356.
[22] Gao Xin Qiang,Rong Gang & Zhu Yong Quan. (2011). Analysis on the Development Trend of the Longitudinal Cracks During Tunnels Construction Based on the Strength Reduction Theory. Advanced Materials Research,368-373(368-373),2949-2954.
[23] Mina Fakeh,Akram Jawdhari & Amir Fam. (2025). Recommended concrete damage plasticity parameters and constitutive models for UHPC in ABAQUS. Engineering Structures,333,120154-120154.
[24] Siddhesh S Kulkarni,Aoun Hussnain,Israr Ud Din & Kamran A Khan. (2025). A simplified finite-strain constitutive model for SMP to simulate foldable and auxetic structures: experiments and numerical implementation in ABAQUS. Smart Materials and Structures,34(4),045004-045004.